



A miniaturized comprehensive approach for total lipidome analysis and vitamin D metabolite quantification in human serum

Danilo Donnarumma¹ · Alessia Arena¹ · Emanuela Trovato¹ · Francesca Rigano¹ · Mariosimone Zoccali² · Luigi Mondello^{1,3}

Received: 30 December 2022 / Revised: 26 April 2023 / Accepted: 12 May 2023
© Springer-Verlag GmbH Germany, part of Springer Nature 2023

Abstract

The balance between the different lipid molecules present in biological fluids accurately reflects the health state of the organism and can be used by medical personnel to finely tune therapy to a single patient, a process known as precision medicine. In this work, we developed a miniaturized workflow for the analysis of different lipid classes at the intact level, as well as their fatty acid constituents, starting from human serum. Fatty acids were identified by using flow-modulated comprehensive gas chromatography coupled to mass spectrometry (FM-GC×GC–MS), and their relative amount as well as the ratio of specific FA classes was determined by using FM-GC×GC with a flame ionization detector. Ultra-high-performance liquid chromatography coupled to tandem mass spectrometry was used for the simultaneous quantification of vitamin D metabolites and assessment of different intact lipid classes. An MRM method was developed for the quantification of five vitamin D metabolites (vitamin D2, vitamin D3, 25-hydroxyvitamin D2, 25-hydroxyvitamin D3, 24R,25-dihydroxyvitamin D3), and validated in terms of LoD, LoQ, accuracy, and precision, also using a certified reference material. At the same time, a combination of SCAN, precursor ion scan, and neutral loss scan, in both positive and negative modes, was used for the identification of 81 intact lipid species, such as phospholipids, cholesteryl esters, and triacylglycerols, in less than 25 min. In order to easily monitor the lipid composition and speed up the identification process, a two-dimensional map of the lipidome was generated, by plotting the molecular weight of the identified molecules versus their retention time. Moreover, a relative quantification was performed within each lipid class identified. The combination of untargeted and targeted data could provide useful information about the pathophysiological condition of the organism and evaluate, in a tailored manner, an efficient action.

Keywords Lipidomic · Vitamin D · Precision medicine · Comprehensive two-dimensional gas chromatography · UHPLC-MS/MS · Fatty acids

Published in the topical collection *Young Investigators in (Bio-) Analytical Chemistry 2023* with guest editors Zhi-Yuan Gu, Beatriz Jurado-Sánchez, Thomas H. Linz, Leandro Wang Hantao, Nongnoot Wongkaew, and Peng Wu.

✉ Mariosimone Zoccali
mariosimone.zoccali@unime.it

¹ Department of Chemical, Biological, Pharmaceutical and Environmental Sciences, University of Messina, 98168 Messina, Italy

² Department of Mathematical and Computer Science, Physical Sciences and Earth Sciences, University of Messina, 98168 Messina, Italy

³ Chromaleont S.R.L., c/o Department of Chemical, Biological, Pharmaceutical and Environmental Sciences, University of Messina, 98168 Messina, Italy

Introduction

Lipidomics is the branch of metabolomics that aims to study all the lipids within a living system or in complex biological samples, known as lipidome [1]. Such lipid metabolites participate in all the major metabolic pathways and biological processes of the organism, regulating the balance between health and disease states. For this reason, lipids are the main candidates for understanding the general health state and correlate it with the lifestyle [2].

Indeed, in clinical research, there are many examples of lipidomic tests used to better understand the disease pathophysiology, discover new biomarkers, identify new potential therapeutic targets, and monitor the patient's response to the therapy. Recent studies have provided insight into the contribution of lipid alteration on several metabolic diseases

(cardiovascular disease [3], diabetes [4], non-alcoholic fatty liver disease (NAFLD) [5, 6]), neurodegenerative disease (Alzheimer's disease [7], multiple sclerosis [8]), cancer [9], and other inflammatory conditions and viral infections, such as asthma [10], atopic dermatitis [11], Fabry disease [12], and COVID-19 infection [13]. Despite the vast literature on this topic, and the promising applications developed, most lipid analyses used in clinical diagnostics focus only on single lipidic biomarkers, or on a very limited subset of molecules. Some examples of such approaches include vitamin D metabolites [14], sex steroid hormones [15, 16], and acylcarnitine panels [17, 18].

In particular, vitamin D deficiency is recognized as a pandemic health concern, connected with a variety of diseases, including cancer [19], autoimmune disease [20], neurological disease [21], metabolic disease [22], and viral infection such as COVID-19 [23]. Both vitamin D major forms, vitamin D₂ (ergocalciferol) and vitamin D₃ (cholecalciferol), can be introduced with the diet or as supplements, whereas only vitamin D₃ can be synthesized in the skin upon exposure to UV light. Both forms need to be processed, first in the liver, in order to obtain the 25-hydroxyvitamin D₂/D₃, collectively known as 25OH-D, and later in the kidney, producing the metabolites 1- α ,25-dihydroxyvitamin-D₃ (1 α ,25(OH)₂-D₃), 1- α ,25-dihydroxyvitamin-D₂ (1 α ,25(OH)₂-D₂), and the minor metabolite, 24R,25(OH)₂-D₃. The mono-hydroxylated forms are the clinically accepted markers to dose vitamin D in human serum, but traditional immunochemical assays used for such scope shows substantial limitations in terms of accuracy and specificity [24], especially in the differentiation of the different vitamin D metabolites. Nowadays, high-pressure liquid chromatography coupled to tandem mass spectrometry (HPLC-MS/MS) is considered the gold standard for the analysis of vitamin D metabolites [14], and for this reason, many clinical laboratories all over the world acquired MS instrumentation. This represents the doorstep for the expansion of their MS-based clinical test portfolios toward other analytes of interest.

In this scenario, lipidomics, with its aim to analyze the total lipid fraction of the sample, offers a unique opportunity to describe, in a systems-wide manner, what is happening in the human body, painting a picture of the ongoing physiological processes, with particular focus on those involved in lipid metabolism and inflammation. Among the possible targets, the importance of the analysis of fatty acids (FAs) in human plasma has been reported in several studies. In fact, by monitoring the FA profile, it is possible to determine dysregulation phenomena strictly related to multiple inflammatory diseases [2, 25, 26]. The FA profile is commonly investigated by using gas chromatography (GC) techniques, after a derivatization procedure, following lipid extraction [2]. However, nowadays, the use of multidimensional chromatographic techniques is increasingly used, even for

routine analysis in clinical study, especially, employing flow modulators characterized by robustness and reduced economical costs [27, 28].

Another strategy in lipidomics applied to clinical analysis focuses on intact lipid investigation. A recent example of such approach is represented by the diagnosis of non-alcoholic fatty liver disease (NAFLD) from non-alcoholic steatohepatitis (NASH) [29]. NASH is a more advanced condition of NAFLD, and may eventually lead to fibrosis, cirrhosis, and hepatocellular carcinoma. Until a few years ago, the gold standard method for discriminating between the two conditions was an invasive liver biopsy. Nowadays, a total of 28 triacylglycerides (TGs), divided into two panels, have been selected: 11 TGs formed the first panel, and could significantly distinguish between normal liver (NL) and NAFLD, but not NASH and NAFLD, whereas the second panel, containing 20 TGs, distinguished between NASH and NAFLD, but not NL from NASH [29].

In this contest, we developed a comprehensive workflow both for the analysis of fatty acids, through flow-modulated comprehensive gas chromatography coupled to mass spectrometry (FM-GC \times GC-MS), and for the fast and simultaneous quantification of vitamin D metabolites and assessment of intact lipids in human serum, by using ultra-high-performance liquid chromatography coupled to tandem mass spectrometry (UHPLC-MS/MS). The established approach takes advantage of analytical instrumentation already available in many clinical laboratories, and expands their portfolio for the analysis of new lipid biomarkers. Finally, particular emphasis was put on the sample preparation in order to reduce as much as possible both the sample volume and the amount of solvents used for the extraction and derivatization of the analytes of interest. The data obtained were used to build lipidomics maps for the fast screening of different lipid classes, to easily read possible lipid alterations, and possibly correlate them with the general health state of the patient.

Materials and methods

Samples, chemicals, and materials

Commercially available reference material SRM 972a "Vitamin D Metabolites in Frozen Human Serum" from National Institute of Standards & Technology (NIST) and serum from one informed donor were used for analytical purpose. Vitamin D₂, vitamin D₃, 25-hydroxyvitamin D₂, 25-hydroxyvitamin D₃, 24R,25-dihydroxyvitamin D₃, vitamin D₂ (6,19,19-d₃), vitamin D₃ (6,19,19-d₃), 25-hydroxyvitamin D₂ (6,19,19-d₃), 25-hydroxyvitamin D₃ (6,19,19-d₃), and 24R,25-dihydroxyvitamin D₃ (26,26,26,27,27,27-d₆) were

purchased from Merck Life Science (Darmstadt, Germany). For the derivatization, CH_3ONa and BF_3 in methanol solution (14% w/v) were employed (Merck Life Science). A $\text{C}_7\text{--C}_{30}$ alkane mixture was purchased from Merck Life Science.

All solvents were purchased from Merck Life Science. Before the analysis, all biological fluids were maintained at $-80\text{ }^\circ\text{C}$, while all standards were maintained at $-20\text{ }^\circ\text{C}$.

Sample preparation for FAME analysis

Fatty acid extraction and derivatization was carried out using the procedure reported by Micalizzi et al. [2]. Briefly, 500 μL of CH_3ONa in methanol (0.5% w/v) was added to 50 mg of human serum and heated for 15 min at $95\text{ }^\circ\text{C}$. After cooling, 500 μL of BF_3 methanolic solution was added to the mixture and heated again for 15 min at $95\text{ }^\circ\text{C}$. The derivatized fatty acids were extracted by adding 350 μL of *n*-heptane and 300 μL of a NaCl saturated solution. The sample was agitated using a vortex mixer and, after gravitational separation of the phases, the upper heptanic FAME layer was recovered for the GC analysis. Three independent extractions were performed.

Sample preparation for intact lipid analysis

Prior to lipid extraction, the serum proteins were precipitated by adding 50 μL of acetonitrile (ACN), containing the internal standard mix, composed of stable isotope labeled (SIL) vitamin D metabolites, at the concentration of 10 ng mL^{-1} , to 50 μL of human serum and kept 10 min at $4\text{ }^\circ\text{C}$. After protein precipitation, the intact lipids were extracted by adding 450 μL of hexane and mixed 10 min at 2500 rpm. The upper organic layer was recovered after centrifugation (5 min, $500\times g$ at $4\text{ }^\circ\text{C}$) and dried out under a gentle stream of nitrogen. Before the analysis, the samples were resuspended in 50 μL of 2-propanol. The same protocol was applied to the four levels of the certified NIST 972a reference material. Three independent extractions were performed for each sample.

Flow-modulated GC \times GC analyses

The separation and identification of the FAMES was achieved through a FM-GC \times GC-MS analysis performed on a GCMS-TQ8040 equipped with a split/splitless injector and an AOC-20i autosampler. A triple quadrupole mass spectrometer was employed in SCAN mode only; the collision cell and the second quadrupole act as fly-through zone only (Shimadzu Corporation, Kyoto, Japan). Data were collected by using the GCMS Solution v.4.52 software (Shimadzu); the ChromSquare v. 2.3 software was used for GC \times GC data processing (Shimadzu). Mass spectral identification

was performed by using the ChromSquare software and the Lipids Mass Spectral Database (John Wiley & Sons, Inc). The ^1D column was an SLB-5 ms $20\text{ m}\times 0.18\text{ mm ID}\times 0.18\text{ }\mu\text{m df}$ (silphenylene polymer virtually equivalent in polarity to poly (5% diphenyl/95% methyl siloxane)). A Supelcowax-10 $5\text{ m}\times 0.32\text{ mm ID}\times 0.25\text{ }\mu\text{m df}$ capillary (poly(ethylene glycol) phase) was used as ^2D column, both were from Merck Life Science (Merck KGaA, Darmstadt, Germany). Modulation was performed by using a 7-port wafer chip equipped with an external accumulation loop with dimensions $20\text{ cm}\times 0.51\text{ mm ID}$ (Chromaleont srl, Messina, Italy). Injection volume was 1.0 μL (splitless mode, 2 min) at $250\text{ }^\circ\text{C}$ injector temperature; He was used as carrier gas. The initial ^1D average linear velocity (ALV) was approx. 20 cm s^{-1} , while the ^2D ALV was approx. 260 cm s^{-1} . The system was operated in the constant flow mode in both the ^1D and ^2D at 0.4 and 8 mL min^{-1} , respectively. Temperature program was as follows: $140\text{ }^\circ\text{C}$ up to $280\text{ }^\circ\text{C}$ at $3\text{ }^\circ\text{C min}^{-1}$; modulation period was 3.2 s (0.4 s re-injection period). As for MS conditions, electron ionization mode (70 eV) was employed. Interface and ion source temperatures were kept at $240\text{ }^\circ\text{C}$ and $200\text{ }^\circ\text{C}$, respectively. Analysis were acquired in SCAN, using a mass range of m/z 45–330 and a 50-Hz spectral production frequency. The quantification of the FAMES was performed using a FM-GC \times GC system coupled to a flame ionization detector (FID) on a Nexis GC-2030 equipped with a split/splitless injector and an AOC-20i autosampler. The same GC \times GC columns setup and analytical condition of the MS one were employed. The FID temperature was set at $300\text{ }^\circ\text{C}$ (sampling rate: 20 ms), while the gas flows were 40 mL min^{-1} for H_2 , 30 mL min^{-1} for the make-up gas (nitrogen), and 400 mL min^{-1} for air. Data were collected and processed using the LabSolution software v.5.92 (Shimadzu).

UHPLC-MS/MS analysis

Intact lipid analysis and vitamin D metabolite quantification were performed by using a Nexera X2 UHPLC system coupled to a LCMS-8060 mass spectrometer (Shimadzu, Duisburg, Germany). Data acquisition and processing was performed using the LabSolutions software (version 5.95 Shimadzu). The separation of the various lipid classes and species was achieved by using an Ascentis Express C18 reverse phase column ($100\times 2.1\text{ mm}$, $2.7\text{ }\mu\text{m}$) (Merck Life Science) and a mobile phase composed of ammonium formate 20 mM in water as solvent A, and a mixture of 2-propanol/acetonitrile/ammonium formate 20 mM in water (60:36:4 v/v/v) with 0.1% formic acid as solvent B. The gradient program was as follows: 0–12 min, 60–100% B, held for 16 min. The flow rate was 0.4 mL min^{-1} ; the column oven was set at $40\text{ }^\circ\text{C}$ and the injection volume was 2 μL . MS and MS/MS acquisitions were performed using ESI source

operating both in positive (+) and negative ionization modes (-), with the following parameters: interface temperature, 450 °C; CDL temperature, 250 °C; heat block temperature, 200 °C; nebulizing gas flow (N₂), 3 L min⁻¹; drying gas flow (N₂), 5 L min⁻¹; acquisition range, 350–1250 m/z in positive mode and 150–1250 m/z in negative mode. Additional MS/MS experiments were optimized through the injection of single PL standards, and the selected events are reported in Rigano et al [30]. Briefly, precursor ion scan analysis was performed for LPC/PC/SM and LPI/PI (diagnostic fragments: 184 m/z in positive mode and 241 m/z in negative mode, respectively), while neutral loss scan was used for LPE/PE, LPS/PS, and LPG/PG (diagnostic fragments: 141 Da and 185 Da in positive mode, and 153 Da in negative mode, respectively). The LIPID MAPS Structure Database (LMSD) was employed for compound identification (available at <https://www.lipidmaps.org/data/structure/>) [31] by searching the following ion type: [M+H]⁺ for cholesterol and cholesteryl esters (CEs), LPC/PC/SM, LPE/PE, and LPS/PS; [M-H]⁻ for LPI/PI and LPG/PG; and [M+NH₄]⁺ for TGs. Vitamin D metabolites, and their respective stable isotope labelled analogue, were detected in multiple reaction monitoring (MRM) acquisition mode by applying specific acquisition windows depending on the retention time of each target, using a dwell time of 15.0 ms, to obtain at least 10 scans per peak, as required for a correct quantification.

Optimization of MRM transitions and method validation

The MRM parameters of vitamin D metabolites, both not labeled and SIL, were optimized in terms of quantifier ion (Q), qualifier ion (q), and collision energy (CE) (Table 1), using the software's automatic procedure, by the direct injection of 2 μL of each standard at concentration 10 mg L⁻¹. The parameters of the ESI (+) ion source were the same as described in the previous paragraph.

The calibration curves were constructed in the range 2.5–100 ng mL⁻¹ (2.5, 5, 10, 25, 50, 75, 100 ng mL⁻¹, with 5 replicates for each point) using the SIL vitamin D metabolites as internal standards at the final concentration of 10 ng mL⁻¹. The quartile approach was used to exclude potential outliers located outside the limits defined as follows:

$$\text{Lower limit} : Q_1 - 1.5 \times \text{IQR} \rightarrow \text{Upper limit} : Q_3 + 1.5 \times \text{IQR}$$

where Q_1 and Q_3 are the first and third quartiles, respectively, and IQR is the interquartile range calculated as the difference between Q_1 and Q_3 .

For each compound, a linear regression study was performed to evaluate the significance of y intercept and the curve was forced to zero when the *P*-value resulted higher than 0.05. To correct the data heteroscedasticity, four different weighting factors ($1/x$; $1/x^2$; $1/y$; $1/y^2$) were tested. Limit of detection (LoD) and limit of quantification (LoQ) were calculated according to Eurachem guidelines [32]. Briefly, LoDs and LoQs were calculated by using the following equations:

$$\text{LoD} = 3 \times s'_0 \quad \text{LoQ} = 10 \times s'_0$$

where s'_0 is the ratio between the standard deviation of the results at the lowest concentration level, and the square root of the number of analysis ($n = 10$). The accuracy of the method was evaluated by analyzing the certified NIST 972a reference material and by comparing the experimental quantitative results with the values reported in the NIST certificate of analysis, and expressed as recovery (R%).

The inter-day repeatability was evaluated as the CV% of the vitamin D metabolites peak areas for the different NIST 972a levels, measured on three non-consecutive days over 2 months ($n = 10$).

Table 1 List of the vitamin D metabolites and their optimized MRM parameters. *Q*, quantifier ion; *q*, qualifier ion; *CE*, collision energy (V); *Q/q* %, qualifier-quantifier ratio; time windows width (min)

Standard	MRM transitions				Time window (min)
	[M+H] ⁺	<i>Q</i> (CE)	<i>q</i> (CE)	<i>q/Q</i> %	
24R,25(OH) ₂ -D3	417.3	381.35 (-11)	399.40 (-11)	94.4	1–1.8
24R,25(OH) ₂ -D3 (d6)	423.3	387.35 (-19)	405.40 (-15)	91.1	
25OH-D3	401.4	383.30 (-11)	365.25 (-12)	37.3	2.4–3.2
25OH-D3 (d3)	404.4	386.30 (-11)	368.25 (-14)	33.4	
25OH-D2	413.4	395.35 (-11)	355.30 (-10)	25.2	2.7–3.5
25OH-D2 (d3)	416.4	398.38 (-11)	358.30 (-10)	29.8	
Vitamin D2	397.4	379.40 (-12)	105.15 (-43)	99.9	8.5–9.3
Vitamin D2 (d3)	400.4	382.40 (-12)	69.05 (-12)	95.4	
Vitamin D3	385.5	367.30 (-13)	259.25 (-16)	75.1	8.6–9.4
Vitamin D3 (d3)	388.5	370.30 (-13)	91.00 (-53)	76.5	

Results and discussion

Untargeted analysis of serum lipidome

Fatty acid profiling in human blood and serum can provide useful information on the lipid metabolic alterations that can be correlated to nutrition status and health conditions. In the present study, a FM-GC × GC-MS method was developed for the FA characterization of a human serum sample, while the quantification was performed using a FM-GC × GC-FID ($n = 3$).

Specifically, the FM-GC × GC-FID was employed to perform a relative quantitation, which cannot be done with a mass spectrometer (due to the different response factors of the different compounds). Within the content of the relative quantitation the use of internal standard it is not mandatory, in fact, any loss during the sample preparation does not lead to a difference in the relative quantitation. Moreover, no discrimination occurred during the injection step due to the limited range of analytes in terms of boiling point (discrimination was evaluated by injecting a C₇-C₃₀ alkane mixture contained at the same concentration).

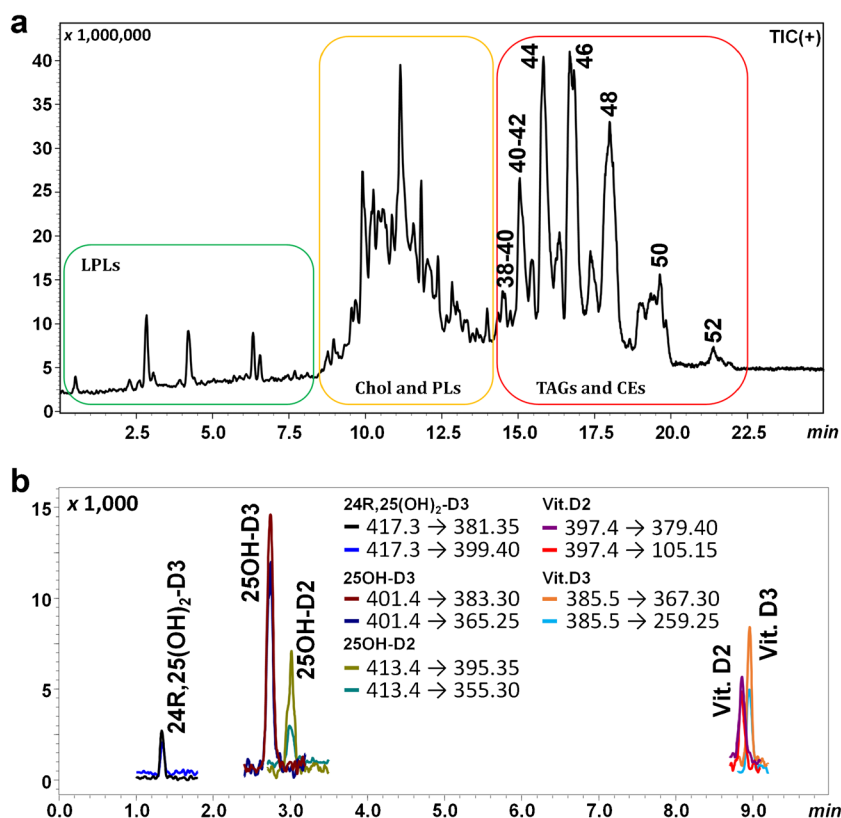
The obtained results expressed in terms of relative percentage (%), FA families (saturated fatty acids (SFA), monosaturated fatty acids (MUFA), polyunsaturated fatty acids (PUFA), ω6, and ω3), and specific FA ratios are reported in Table 2. In fact, as reported in a previous study by Ferracane et al., specific FA ratios are monitored to highlight pathological changes in a patient, as in the case of the ω6/ω3 ratio, a value higher of the optimal range indicates a proinflammatory condition [33, 34]. In the investigated case, the ω3 value was lower compared to the value reported by Harris, able to show a cardioprotective activity [25], while, the ω6/ω3 ratio was higher of the optimal range, thus indicating a proinflammatory condition [34].

On the other hand, by monitoring the intact lipids that directly reflect the lipid metabolism regulation in response to exogenous stimuli, it is possible to obtain insights into the perturbation of essential metabolic processes in which each species is involved. The untargeted UHPLC-MS/MS approach allowed the identification of 81 lipidic molecules separated according to their polarity (Table S1) and eluted by increasing partition number (PN), calculated using the equation $PN = CN - 2DB$, where CN and DB are the carbon number and the double bond number of the FA constituents, respectively. The obtained chromatogram can be divided into three regions: very polar lipids (LPLs), medium-polar lipids (PLs and free cholesterol (Chol)), and non-polar lipids (TGs and CEs), eluted in the PN range 38–52 (Fig. 1a). The total list of the identified molecules is reported in Table S1 as well as their retention time (t_R),

Table 2 Fatty acid methyl ester levels, expressed as area percentages along with their CV% ($n = 3$), and specific ratios

FAME	Area (%)	CV%
Myristic acid (C14:0)	0.18	3.6
Pentanoic acid (C15:0)	0.17	1.4
Palmitoleic acid (C16:1ω9)	0.32	1.6
Palmitoleic acid (C16:1ω7)	0.93	4.7
Palmitic acid (C16:0)	21.70	0.4
Heptadecanoic acid (C17:0)	0.42	4.9
γ-Linolenic acid (C18:3ω6)	0.47	4.8
Linoleic acid (C18:2ω6)	30.00	0.1
Oleic acid (C18:1ω9)	24.88	0.6
Vaccenic acid (C18:1ω7)	1.66	1.0
Stearic acid (C18:0)	7.34	0.9
Arachidonic acid (C20:4ω6)	8.22	0.5
Eicosapentaenoic acid (C20:5ω3)	0.39	4.5
Eicosatrienoic acid (C20:3ω6)	1.59	3.0
Docosapentaenoic acid (C22:5ω6)	0.23	0.6
Docosahexaenoic acid (C22:6ω3)	0.71	1.6
Adrenic acid (C22:4ω6)	0.20	2.8
Docosapentaenoic acid (C22:5ω3)	0.18	0.2
Lignoceric acid (C24:0)	0.31	3.6
Nervonic acid (C24:1)	0.09	4.9
SFAs	38.11	-
36.52–41.90		
MUFAs	27.89	-
24.62–31.22		
PUFAs	41.99	-
29.29–36.45		
ω6	40.72	-
25.73–32.63		
ω3	1.27	-
< 4 <i>undesirable</i>		
4–8 <i>intermediate</i>		
> 8 <i>desirable</i>		
ω6/ω3	31.94	-
3.5–5.5		
C18:0/C18:1ω9	0.30	-
< 0.7 <i>hyperactivity</i>		
> 1.3 <i>hypoactivity</i>		
C16:0/C16:1ω7	23.21	-
< 45 <i>hyperactivity</i>		
> 132 <i>hypoactivity</i>		
C18:2ω6/C20:3ω6	18.85	-
< 5 <i>hyperactivity</i>		
> 8 <i>hypoactivity</i>		
C20:4ω6/C20:3ω6	5.17	-
< 6 <i>hypoactivity</i>		
> 9 <i>hyperactivity</i>		

Fig. 1 (a) UHPLC-MS/MS total ion current chromatograms (positive ion mode) of total lipid extract from human serum. The chromatogram can be divided into three regions: very polar lipids (LPLs), medium-polar lipids (PLs and free cholesterol (Chol)), and non-polar lipids (TGs and CEs), eluted in the PN range 38–52. (b) MRM chromatogram of the vitamin D metabolites eluted in the first 10 min. In the inset are reported transition for the different species



detected ions, class, PN, CN, and DB values. Triacylglycerols were present as ammonium and sodium adduct, while phospholipids were detected mainly as protonated (for LPC/PC/SM, LPE/PE and LPS/PS) or deprotonated (for LPI/PI and LPG/PD) ions. Finally, Chol was present as dehydrated ion, while cholesteryl esters were identified using the protonated ion in positive mode, and the deprotonated FA fragment, formed during in source dissociation of the ester, in negative mode.

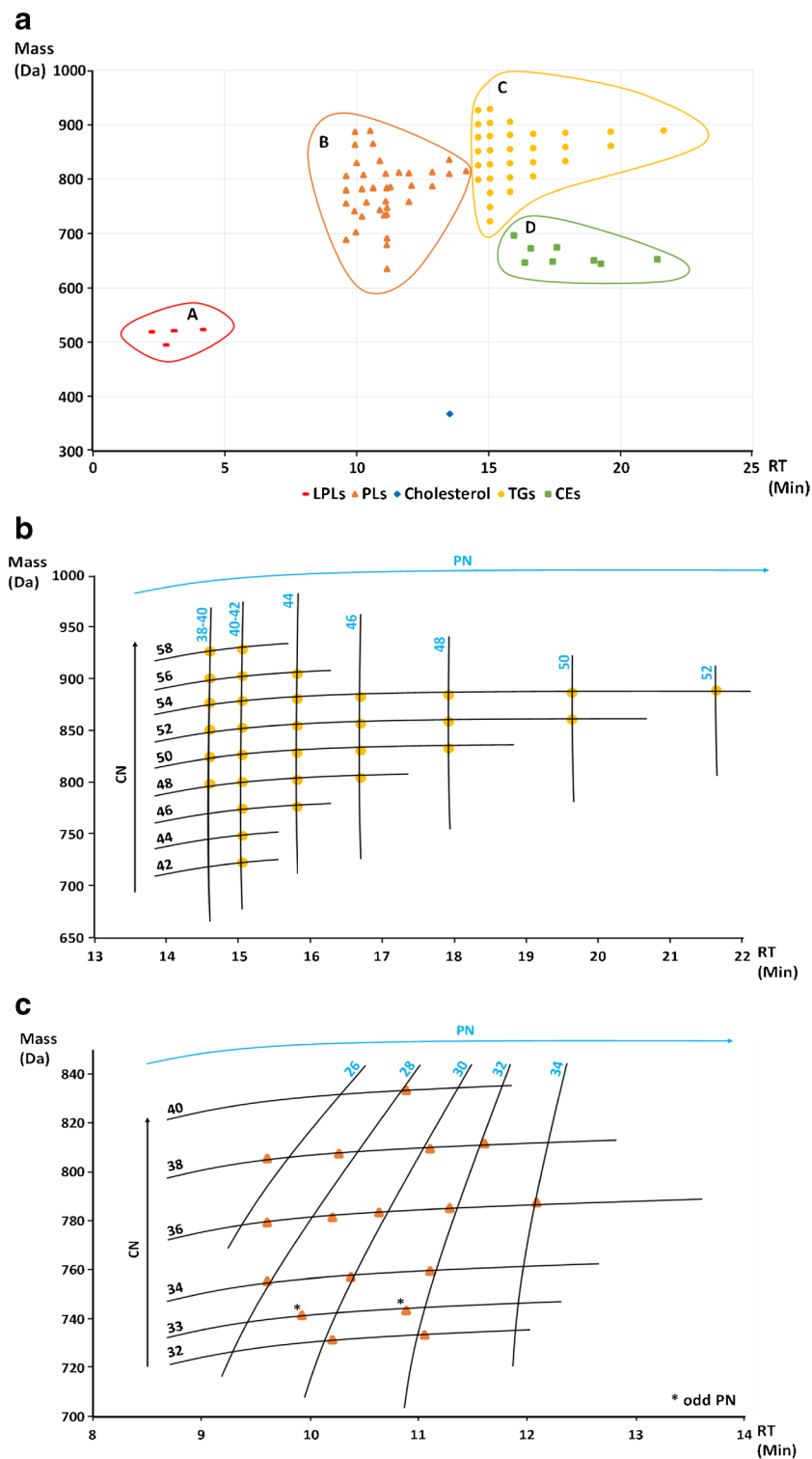
Regarding the polar lipids, it was possible to identify 41 species belonging to 6 different families: 4 LPC, 17 PC, 7 SM, 6 PS, 3 PE, and 4 PI. In addition to LPLs and PLs, it was possible to identify 31 TGs, 8 CEs, as well as cholesterol itself. The number of identified lipids is in agreement with the results published in the most recent years, considering a non-targeted and fast lipidomic method [35–37]. It is noteworthy that vitamin D metabolites are eluted under the region of very polar lipid compounds, but due to their very low concentration levels in real samples, they cannot be detected in SCAN analysis. Their MRM chromatogram is shown in Fig. 1b.

The molecular weight of the identified species and their retention time were used to build a lipidomic map (Fig. 2a) in which it is clearly possible to separate the various species in 4 main regions (A, B, C, and D on the graph, Fig. 2a). In particular, region A contains the LPLs, region B includes the PLs, region C contains the TGs, and finally region D

includes the CEs. Cholesterol is present on the graph as a separated spot in the bottom part of the map, around 13.5 min. From the map, it is immediately possible to separate partially coeluting species, as TGs and CEs, based on differences in their MS data. The developed method, even though much more faster compared to the approaches usually applied for TG separation [38, 39], allowed their elution according to PN and CN, as shown in Fig. 2a, and in more detail in Fig. 2b, greatly simplifying their identification. The same approach can be used for the different class of phospholipids. In Fig. 2c, the map of the PCs is reported, as the most abundant class of PLs identified in the sample. Also in this case, PCs are separated according to their CN and PN, but their elution from the RP column is affected by the equilibrium between the polar head and the non-polar tails. This translates in a different elution pattern, especially in regard of the PN, compared to TGs. Basically, species at the same PN are connected through diagonal lines, instead of the straight lines clearly visible for the TG elution pattern (Fig. 2b).

Such a map can be extremely useful to easily identify the lipidic molecules present in a biological sample. Moreover, in the near future, the application of multivariate statistical methods and/or accurate quantitative methods to the analysis of a larger number of samples, classified according to different pathophysiological conditions, could be meaningful to detect quali-quantitative differences among a large

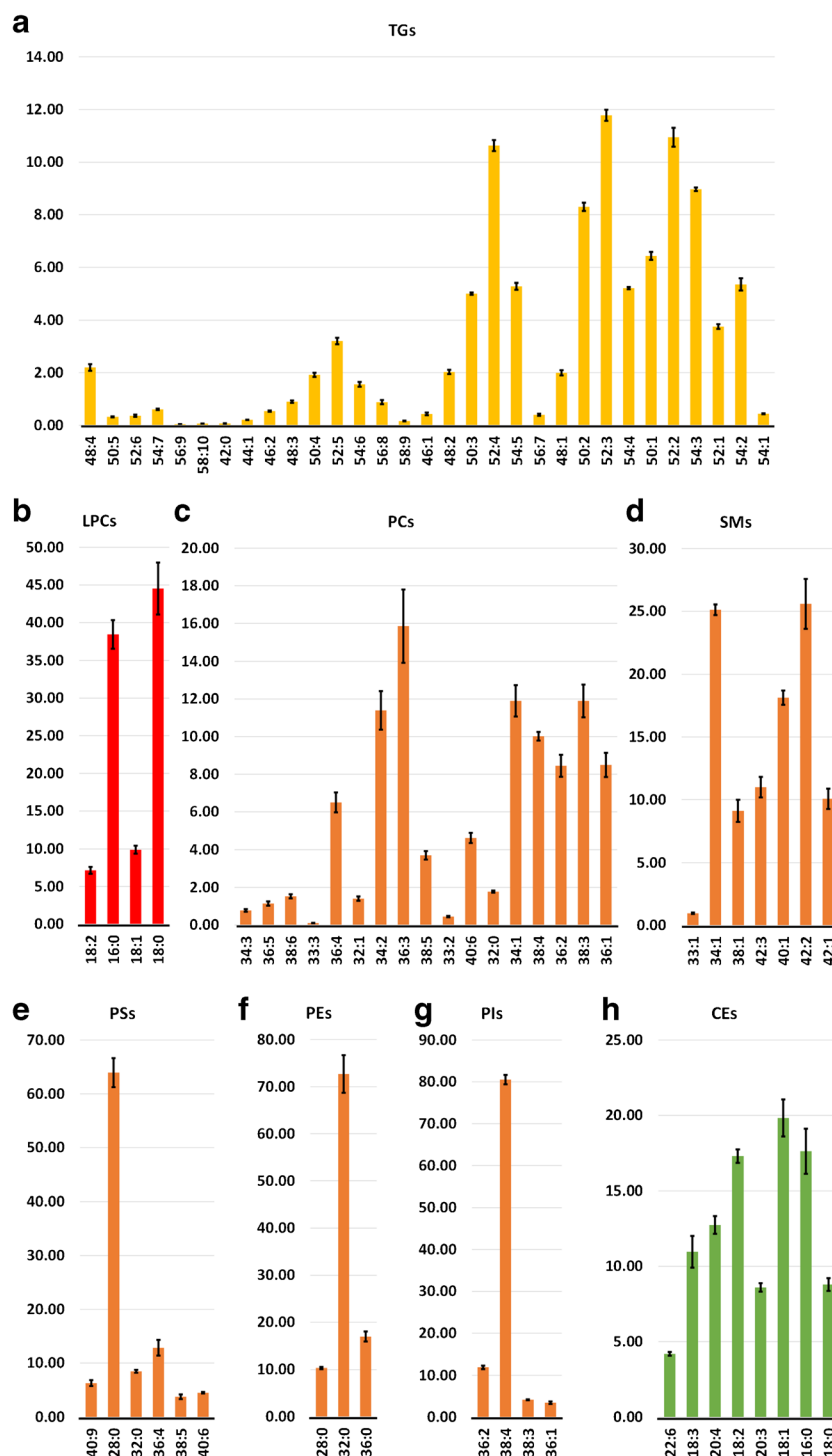
Fig. 2 (a) Map of the intact lipids identified in the serum sample constructed by plotting the molecular weight of each molecule with its retention time. Each lipidic family is clustered in 4 main regions (A, lysophospholipids; B, phospholipids; C, triacylglycerols; D, cholesteryl esters). Cholesterol is reported as a separated spot in the bottom part of the map. (b) Magnification of the TG region of the map with reported CN and PN of the identified molecules. (c) Magnification of the phosphatidylcholine region of the map with reported CN and PN of the identified molecules



population. In order to demonstrate that the method is also suitable for quantitative analysis, a relative quantification within each lipid class (TGs, CEs, SMs, each PL class, and LPCs) was carried out and the inter-day precision was evaluated. Since the relative quantification is performed within each lipid class, we supposed a very similar MS response,

as well as the same recovery during the extraction procedure; then internal standards were not added. The results are shown in Table S1 (% Area and inter-day CV%) and Fig. 3. In particular, Fig. 3a shows the histogram relative to the percentage content of TGs, according to increasing retention time. Major TG components (% > 10%) are those

Fig. 3 Histograms relative to the percentage content of TGs (a), LPCs (b), PCs (c), SM (d), PSs (e), PEs (f), PIs (g), and CEs (h), reported according to increasing retention time. For each identified species, the error bars indicate the inter-day precision



characterized by a carbon number of 52 and double bonds ranging from 2 to 4, being most likely the combination of the most abundant FAs resulting from the GC analysis (palmitic or P, linoleic or L, and oleic or O acids, combined to compose PLL, PLO, and POO). Similarly, the most abundant PC resulted to be PC (36:3), which is probably the combination of oleic and linoleic acid, accounting for more than 50% of

the total FA composition. Interestingly, only saturated FAs were identified in PEs, being PE (32:0) the most abundant one. Arachidonic acid was also putatively found in many complex lipids, especially in the PL structures, such as PS (36:4) and PI (38:4), being it an omega-6 FA correlated to possible alteration of the lipid metabolism. Indeed, this kind of considerations can become meaningful if the lipidomic

study will be extended to a significant number of subjects, which will be the object of a future work. Finally, even if the identification at the level of intact lipids does not provide any indication about the stereo-specificity of the identified analytes, the complementarity of the information arising from LC and GC×GC analysis represents a valid tool to identify the most probable FA combination within each lipid species or, in other terms, the intact lipid structures where FAs are most represented in the human serum.

Targeted quantification of vitamin D metabolites

The low ionization efficiency of vitamin D metabolites is a well-known analytical challenge when measuring vitamin D by LC–MS/MS. For this reason, many developed methods include a derivatization step [14]. In this work, we decided to avoid any derivatization, as required by the green analytical chemistry principles [40]. MRM transitions were then optimized by using both procedures suggested by the Lab-Solutions software: “from precursor ion search” and “from product ion search”. In Table 1, the MRM transitions are reported, with the precursor ion $[M + H]^+$, Q and q ions, CE for both transitions, the quantifier to qualifier ratio (Q/q %), and the acquisition time windows. Despite the product ions, both Q and q corresponded in most cases to the loss of one or two H_2O molecules, which is a common phenomenon in LC–MS ionization mechanisms; the specificity is guaranteed by the coelution of the stable isotope labeled standards, as well as the repeatability of the q/Q ratio. Moreover, the same MRM transitions have been already used in previous works [41–43].

Calibration curves of the vitamin D metabolites were built in the range 2.5–100 ng mL⁻¹ by using the SIL vitamin D metabolites as internal standards. The data scedasticity was tested using the F -test (one tail), and all compounds resulted heteroscedastic. For this reason, it was necessary to apply a weighting factor in order to correct the bias caused by the larger variance of the higher concentrations. For each compound, four different weighting factors ($1/x$; $1/x^2$; $1/y$; $1/y^2$) were tested, and the relative error ($RE\%$) was calculated as follows:

$$RE\% = \frac{C_{\text{exp}} - C_{\text{th}}}{C_{\text{th}}} \times 100$$

where C_{exp} is the concentration calculated using the weighting factor, while C_{th} is the theoretical concentration. The selection of the weighting factor was guided by the minimization of the sum of the $RE\%$ calculated for each point of the calibration curve. In this case, $1/y^2$ was the best choice for all the metabolites. Putative outliers were identified and removed, using the quartile method, and the curves were used to calculate LoD and LoQ, following the Eurachem

guidelines [32], as reported in Table 3. The four levels of the certified NIST 972a reference material were used to calculate accuracy and inter-day precision of the method, expressed as recovery ($R\%$) and CV%, respectively, for the metabolites 25OH-D2, 25OH-D3, and 24R,25(OH)₂-D3 (Table 3). Both parameters resulted satisfactory, with $R\%$ ranging from 98.0% (25OH-D2 in NIST 972a Lv3) to 115.1% (24R,25(OH)₂-D3 in NIST 972a Lv4), and CV% ranging from 3.0 to 10.9%. The values for 25OH-D3 reported in Table 3 are inclusive of the epimeric form (3-*epi*-25OH-D3). Some HPLC–MS/MS methods are present in the literature that focus on the separation between 25OH-D3 and 3-*epi*-25OH-D3, but do not provide any information about other lipidic molecules.

When the developed method was applied to the serum sample from the healthy donor, only vitamin D3 and 25OH-D3 were successfully detected and quantified, with concentrations of 9.75 ± 0.29 ng mL⁻¹ and 32.27 ± 0.24 ng mL⁻¹, respectively, while 24R,25(OH)₂-D3 resulted to be below LoD levels. Even if the absence of vitamin D2 and its metabolites indicates a diet poor of vegetables and mushrooms, the amount of 25OH-D3 is well above the limit of 20 ng mL⁻¹ indicated by the USA Institute of Medicine as insufficiency threshold [44], as well as the higher limit of 30 ng mL⁻¹ set by the Endocrine Society [45].

Conclusions

Several studies already demonstrated that the alteration of the lipid profile may be related to diseases such as diabetes, cancer, and cardiovascular diseases. Therefore, a complete lipidomic analysis, that allows to quickly obtain information on the imbalance of the different lipid classes, can provide valuable information on a patient health state in relation to his lifestyle. Among the different lipidic molecules, of particular interest are the liposoluble vitamins like vitamin D. In the last years, the request for analysis of vitamin D and its metabolites has grown exponentially, given the enormous benefits associated with it, and the serious deficiency that is observed in modern society.

In this work, two analytical methods, based on FM-GC×GC–MS and UHPLC–MS/MS, were developed to quantify the main vitamin D metabolites, and simultaneously evaluate the total lipidome of a subject, starting from a small amount of serum, in terms of intact lipids and their fatty acid components. The quantification method developed for vitamin D metabolites has been validated in terms of LoD, LoQ, accuracy, and precision, with satisfactory values.

The evaluation of specific FA ratios, monitored through FM-GC×GC–MS, allowed to get precious information about the health state of a patient. For example, the high value observed in the sample, compared to the optimal one, for

Table 3 Method validation for vitamin D metabolite calibration curves, corrected by weighting factors. *LoD*, limit of detection; *LoQ*, limit of quantification; *R%*, recovery; *CV%*, coefficient of variation

	24R,25(OH) ₂ -D3	25OH-D3	25OH-D2	Vitamin D3	Vitamin D2
LoD (ng mL ⁻¹)	0.5	0.43	0.51	0.34	0.33
LoQ (ng mL ⁻¹)	1.67	1.44	1.7	1.14	1.10
<i>R</i> ²	0.995	0.997	0.994	0.992	0.991
Linearity range (ng mL ⁻¹)	2–100	2.5–100	2.5–100	2.5–100	2.5–100
Weighting factor	1/ <i>y</i> ²	1/ <i>y</i> ²	1/ <i>y</i> ²	1/ <i>y</i> ²	1/ <i>y</i> ²
NIST SRM972a Lv1					
Cert/ref value (ng mL ⁻¹)	2.66 ± 0.10 ^a	30.61 ± 1.20 ^a	0.54 ± 0.06 ^b	-	-
Measured value (ng mL ⁻¹)	2.95 ± 0.32	31.28 ± 2.52	<LoQ	-	-
<i>R%</i>	110.8	102.2	-	-	-
<i>CV%</i>	10.9	8.1	-	-	-
NIST SRM972a Lv2					
Cert/ref value (ng mL ⁻¹)	1.41 ± 0.05 ^a	19.38 ± 0.49 ^a	0.81 ± 0.06 ^a	-	-
Measured value (ng mL ⁻¹)	<LoQ	20.91 ± 0.64	<LoQ	-	-
<i>R%</i>	-	107.9	-	-	-
<i>CV%</i>	-	3.0	-	-	-
NIST SRM972a Lv3					
Cert/ref value (ng mL ⁻¹)	1.62 ± 0.06 ^a	20.97 ± 0.54 ^{a+b}	13.2 ± 0.3 ^a	-	-
Measured value (ng mL ⁻¹)	<LoQ	21.84 ± 1.27	12.93 ± 1.07	-	-
<i>R%</i>	-	104.2	98.0	-	-
<i>CV%</i>	-	5.8	8.3	-	-
NIST SRM972a Lv4					
Cert/ref value (ng mL ⁻¹)	2.64 ± 0.09 ^a	55.4 ± 3.1 ^a	0.55 ± 0.10 ^b	-	-
Measured value (ng mL ⁻¹)	3.04 ± 0.10	55.31 ± 3.62	<LoQ	-	-
<i>R%</i>	115.1	99.8	-	-	-
<i>CV%</i>	3.3	6.6	-	-	-

the $\omega 6/\omega 3$ ratio indicates a proinflammatory state. Moreover, by UHPLC-MS/MS, it was possible to successfully separate and identify 81 different intact lipid species, belonging to different classes such as phospholipids, cholesteryl esters, and triacylglycerols, in less than 25 min. The data were used to generate a map of the lipidome by plotting the molecular weight of the identified molecules versus their retention time, and a relative quantification within each lipid class (TGs, CEs, SMs, each PL class, and LPCs) was carried out.

In conclusion, the aim of this work was the development of rapid and efficient analytical methods for the fast screening of multiple lipid classes, including vitamin D metabolites, intact lipids, and total FA composition. Finally, the generated lipidomic map, in combination with the FA analysis and vitamin D metabolite quantification, could be successfully used in clinics to monitor any imbalances among the different lipidic species, and promptly intervene with targeted actions if necessary.

Supplementary Information The online version contains supplementary material available at <https://doi.org/10.1007/s00216-023-04756-x>.

Acknowledgements The authors thank Merck Life Science and Shimadzu Corporations for their continuous support. The research was

conducted within the PRIN 2017 “Cutting-edge analytical chemistry methodologies and bio-tools to boost precision medicine in hormone-related diseases” supported by the Ministry University and Scientific Research, Prot. 2017Y2PAB8a.

Author contribution Danilo Donnarumma: conceptualization, investigation, methodology, validation, writing — original draft. Alessia Arena: investigation, methodology, writing — original draft. Emanuela Trovato: investigation, methodology, writing — original draft. Francesca Rigano: conceptualization, methodology, writing — review and editing. Mariosimone Zoccali: conceptualization, methodology, writing — review and editing. Luigi Mondello: conceptualization, funding acquisition, resources, writing — review and editing.

Declarations

Source of biological material The human serum sample was obtained from a single anonymized subject for analytical testing purpose. All procedures followed were in accordance with the ethical standards of the responsible committee on human experimentation (institutional and national) and with the Helsinki Declaration of 1975 (in its most recently amended version). Informed consent was obtained from all individual participants included in the study.

Conflict of interest The authors declare that they have no conflict of interest. The author Luigi Mondello is an editor of this journal but was not involved in the peer review of this article.

References

- Navas-Iglesias N, Carrasco-Pancorbo A, Cuadros-Rodríguez L. From lipids analysis towards lipidomics, a new challenge for the analytical chemistry of the 21st century. Part II: Analytical lipidomics. *TrAC - Trends Anal Chem.* 2009;28:393–403. <https://doi.org/10.1016/j.trac.2008.12.004>.
- Micalizzi G, Ragosta E, Farnetti S, Dugo P, Tranchida PQ, Mondello L, Rigano F. Rapid and miniaturized qualitative and quantitative gas chromatography profiling of human blood total fatty acids. *Anal Bioanal Chem.* 2020;412:2327–37. <https://doi.org/10.1007/s00216-020-02424-y>.
- McGranaghan P, Kirwan JA, Garcia-Rivera MA, Pieske B, Edelman F, Blaschke F, Appunni S, Saxena A, Rubens M, Veledar E, Trippel TD (2021) Lipid metabolite biomarkers in cardiovascular disease: discovery and biomechanism translation from human studies. *Metabolites* 2021;11:1–26.
- Alesi S, Ghelani D, Rassie K, Mousa A. Molecular sciences metabolomic biomarkers in gestational diabetes mellitus: a review of the evidence. *Int J Mol Sci.* 2021;22:5512. <https://doi.org/10.3390/ijms>.
- Vvedenskaya O, Rose TD, Knittelfelder O, Palladini A, Wodke JAH, Schuhmann K, Ackerman JM, Wang Y, Has C, Brosch M, Thangapandi VR, Buch S, Züllig T, Hartler J, Köfeler HC, Röcken C, Coskun Ü, Klipp E, von Schoenfels W, Gross J, Schafmayer C, Hampe J, Pauling JK, Shevchenko A. Nonalcoholic fatty liver disease stratification by liver lipidomics. *J Lipid Res* 2021;62:1–14. <https://doi.org/10.1016/j.jlr.2021.100104>.
- He D, Su Y, Meng D, Wang X, Wang J, Ye H. A pilot study optimizing metabolomic and lipidomic acquisition in serum for biomarker discovery in nonalcoholic fatty liver disease. *J Mass Spectrom Adv Clin Lab.* 2021;22:17–25. <https://doi.org/10.1016/j.jmsacl.2021.10.001>.
- Kim J, Jeong Y. Augmentation of sensory-evoked hemodynamic response in an early Alzheimer's disease mouse model. *J Alzheimer's Dis.* 2013;37:857–68. <https://doi.org/10.3233/JAD-121900>.
- Ferreira HB, Melo T, Monteiro A, Paiva A, Domingues P, Domingues MR. Serum phospholipidomics reveals altered lipid profile and promising biomarkers in multiple sclerosis. *Arch Biochem Biophys* 2021;697:108672. <https://doi.org/10.1016/j.abb.2020.108672>.
- Agarwala PK, Aneja R, Kapoor S. Lipidomic landscape in cancer: actionable insights for membrane-based therapy and diagnoses. *Med Res Rev.* 2022;42:983–1018.
- Wang S, Tang K, Lu Y, Tian Z, Huang Z, Wang M, Zhao J, Xie J. Revealing the role of glycerophospholipid metabolism in asthma through plasma lipidomics. *Clin Chim Acta.* 2021;513:34–42. <https://doi.org/10.1016/j.cca.2020.11.026>.
- Wang H, Cui L, Jia Y, Gao Y, Zhang G, He C. Application of lipidomics to reveal differences of facial skin surface lipids between atopic dermatitis and healthy infants. *J Cosmet Dermatol.* 2020;19:1528–34. <https://doi.org/10.1111/jocd.13188>.
- Yazd HS, Bazargani SF, Vanbeek CA, King-Morris K, Heldermon C, Segal MS, Clapp WL, Garrett TJ. LC-MS lipidomics of renal biopsies for the diagnosis of Fabry disease. *J Mass Spectrom Adv Clin Lab.* 2021;22:71–8. <https://doi.org/10.1016/j.jmsacl.2021.11.004>.
- Song JW, Lam SM, Fan X, Cao WJ, Wang SY, Tian H, Chua GH, Zhang C, Meng FP, Xu Z, Fu JL, Huang L, Xia P, Yang T, Zhang S, Li B, Jiang TJ, Wang R, Wang Z, Shi M, Zhang JY, Wang FS, Shui G. Omics-driven systems interrogation of metabolic dysregulation in COVID-19 pathogenesis. *Cell Metab.* 2020;32:188–202.e5. <https://doi.org/10.1016/j.cmet.2020.06.016>.
- Zelzer S, Goessler W, Herrmann M. Measurement of vitamin D metabolites by mass spectrometry, an analytical challenge. *J Lab Precis Med* 2018;3:99. <https://doi.org/10.21037/jlpm.2018.11.06>.
- Lacey JM, Minutti CZ, Magera MJ, Tauscher AL, Casetta B, McCann M, Lymp J, Hahn SH, Rinaldo P, Matern D. Improved specificity of newborn screening for congenital adrenal hyperplasia by second-tier steroid profiling using tandem mass spectrometry. *Clin Chem.* 2004;50:621–5. <https://doi.org/10.1373/clinchem.2003.027193>.
- Gaudl A, Kratzsch J, Ceglarek U. Advancement in steroid hormone analysis by LC-MS/MS in clinical routine diagnostics – a three year recap from serum cortisol to dried blood 17 α -hydroxyprogesterone. *J Steroid Biochem Molec Biol* 2019;192:105389. <https://doi.org/10.1016/j.jsbmb.2019.105389>.
- Janzen N, Hofmann AD, Schmidt G, Das AM, Illsinger S. Non-invasive test using palmitate in patients with suspected fatty acid oxidation defects: disease-specific acylcarnitine patterns can help to establish the diagnosis. *Orphanet J Rare Dis* 2017;12:187. <https://doi.org/10.1186/s13023-017-0737-7>.
- Miller MJ, Cusmano-Ozog K, Oglesbee D, Young S. Laboratory analysis of acylcarnitines, 2020 update: a technical standard of the American College of Medical Genetics and Genomics (ACMG). *Genet Med.* 2021;23:249–58. <https://doi.org/10.1038/s41436>.
- Cook NR. Vitamin D and cancer: can we believe the evidence from observational studies? *Clin Chem.* 2013;59:726–8.
- Priehl B, Treiber G, Pieber TR, Amrein K. Vitamin D and immune function. *Nutrients.* 2013;5:2502–21.
- Janjusevic M, Gagno G, Fluca AL, Padoan L, Beltrami AP, Sinagra G, Moretti R, Aleksova A. The peculiar role of vitamin D in the pathophysiology of cardiovascular and neurodegenerative diseases. *Life Sci* 2022;289:120193. <https://doi.org/10.1016/j.lfs.2021.120193>.
- Park JE, Pichiah PBT, Cha YS. Vitamin D and metabolic diseases: growing roles of vitamin D. *J Obes Metab Syndr.* 2018;27:223–32.
- Banerjee A, Ganguly U, Saha S, Chakrabarti S, Saini RV, Rawal RK, Saso L, Chakrabarti S. Vitamin D and immuno-pathology of COVID-19: many interactions but uncertain therapeutic benefits. *Expert Rev Anti Infect Ther.* 2021;19:1245–58.
- Vogeser M. Quantification of circulating 25-hydroxyvitamin D by liquid chromatography-tandem mass spectrometry. *J Steroid Biochem Mol Biol.* 2010;121:565–73.
- Harris WS. Omega-3 fatty acids and cardiovascular disease: a case for omega-3 index as a new risk factor. *Pharmacol Res.* 2007;55:217–23.
- Külzow N, Witte AV, Kerti L, Grittner U, Schuchardt JP, Hahn A, Flöel A. Impact of omega-3 fatty acid supplementation on memory functions in healthy older adults. *Journal of Alzheimer's Disease.* 2016;51:713–25. <https://doi.org/10.3233/JAD-150886>.
- Zanella D, Henin A, Mascrez S, Stefanuto PH, Franchina FA, Focant JF, Purcaro G. Comprehensive two-dimensional gas chromatographic platforms comparison for exhaled breath metabolites analysis. *J Sep Sci.* 2022. <https://doi.org/10.1002/jssc.202200164>.
- Aloisi I, Giocastro B, Ferracane A, Salerno TMG, Zoccali M, Tranchida PQ, Mondello L. Preliminary observations on the use of a novel low duty cycle flow modulator for comprehensive two-dimensional gas chromatography. *J Chromatogr A* 2021;1643:462076. <https://doi.org/10.1016/j.chroma.2021.462076>.
- Mayo R, Crespo J, Martínez-Arriaga I, Banales JM, Arias M, Mincholl I, Aller de la Fuente R, Jiménez-Ag R, Alonso C, de Luis DA, Vitek L, Stritesky J, Caballería J, Romero-Gomez M, Martínez-Duce A, María Mug J, Huguet Uerza, Ignacio Busteros-Moraza J, Idowu MO, Castro A, Luz Martínez-Chantar M, Ortiz P, Bruha R, Lu SC, Bedossa P, Noureddin M, Sanyal AJ, Mato JM. Metabolomic-based noninvasive serum test to diagnose nonalcoholic steatohepatitis: results from discovery and validation

- cohorts. *Hepatol Commun* 2018;2:807–820. <https://doi.org/10.1002/hep4.1188/full>.
30. Rigano F, Arena P, Mangraviti D, Donnarumma D, Dugo P, Donato P, Mondello L, Micalizzi G. Identification of high-value generating molecules from the wastes of tuna fishery industry by liquid chromatography and gas chromatography hyphenated techniques with automated sample preparation. *J Sep Sci*. 2021;44:1571–80. <https://doi.org/10.1002/jssc.202100108>
 31. Sud M, Fahy E, Cotter D, Brown A, Dennis EA, Glass CK, Merrill AH, Murphy RC, Raetz CRH, Russell DW, Subramaniam S. LMSD: LIPID MAPS structure database. *Nucleic Acids Res* 2007;35:527–532. <https://doi.org/10.1093/nar/gkl838>.
 32. Magnusson B, Örnemark U. The fitness for purpose of analytical methods : a laboratory guide to method validation and related topics. Eurachem Guide Eurachem Guide. 2014. Available from <http://www.eurachem.org>
 33. Ferracane A, Aloisi I, Galletta M, Zoccali M, Tranchida PQ, Micalizzi G, Mondello L. Automated sample preparation and fast GC–MS determination of fatty acids in blood samples and dietary supplements. *Anal Bioanal Chem*. 2022;414:8426–8435. <https://doi.org/10.1007/s00216-022-04379-8>.
 34. Ferreri C, Chatgililoglu C. Membrane lipidomics for personalized health. 1st ed. John Wiley & Sons, 2015.
 35. Zhang F, Zhang Q, Liu X, Gao M, Li X, Wang Y, Chang Y, Zhang X, Huo Z, Zhang L, Shan J, Zhu B, Yao W. Human serum lipidomics analysis revealed glyphosate may lead to lipid metabolism disorders and health risks. *Environ Int* 2023;171:107682. <https://doi.org/10.1016/j.envint.2022.107682>.
 36. Yang L, Wang L, Deng Y, Sun L, Lou B, Yuan Z, Wu Y, Zhou B, Liu J, She J. Serum lipids profiling perturbances in patients with ischemic heart disease and ischemic cardiomyopathy. *Lipids Health Dis* 2020;19. <https://doi.org/10.1186/s12944-020-01269-9>.
 37. Djekic D, Pinto R, Repsilber D, Hyotylainen T, Henein M. Serum untargeted lipidomic profiling reveals dysfunction of phospholipid metabolism in subclinical coronary artery disease. *Vasc Health Risk Manag*. 2019;15:123–35. <https://doi.org/10.2147/VHRM.S202344>.
 38. Rigano F, Oteri M, Micalizzi G, Mangraviti D, Dugo P, Mondello L. Lipid profile of fish species by liquid chromatography coupled to mass spectrometry and a novel linear retention index database. *J Sep Sci*. 2020;43:1773–80. <https://doi.org/10.1002/jssc.2020010171>.
 39. Causevic A, Olofsson K, Adlercreutz P, Grey C. Non-aqueous reversed phase liquid chromatography with charged aerosol detection for quantitative lipid analysis with improved accuracy. *J Chromatogr A* 2021;1652:462374. <https://doi.org/10.1016/j.chroma.2021.462374>.
 40. Anastas P, Eghbali N. Green chemistry: principles and practice. *Chem Soc Rev*. 2010;39:301–12. <https://doi.org/10.1039/b918763b>.
 41. Maunsell Z, Wright DJ, Rainbow SJ. Routine isotope-dilution liquid chromatography-tandem mass spectrometry assay for simultaneous measurement of the 25-hydroxy metabolites of vitamins D2 and D3. *Clin Chem*. 2005;51:1683–90. <https://doi.org/10.1373/clinchem.2005.052936>.
 42. Chen H, McCoy LF, Schleicher RL, Pfeiffer CM. Measurement of 25-hydroxyvitamin D3 (25OHD3) and 25-hydroxyvitamin D2 (25OHD2) in human serum using liquid chromatography-tandem mass spectrometry and its comparison to a radioimmunoassay method. *Clin Chim Acta*. 2008;391:6–12. <https://doi.org/10.1016/j.cca.2008.01.017>.
 43. Sohail A, Al Menhali A, Hisaindee S, Shah I. An lc-ms/ms method for analysis of vitamin d metabolites and c3 epimers in mice serum: oral supplementation compared to UV irradiation. *Molecules* 2021;26:5182. <https://doi.org/10.3390/molecules26175182>.
 44. Institute of Medicine. Dietary reference intakes for calcium and vitamin D. National Academies Press. 2011. <https://doi.org/10.17226/13050>.
 45. Holick MF, Binkley NC, Bischoff-Ferrari HA, Gordon CM, Hanley DA, Heaney RP, Murad MH, Weaver CM. Evaluation, treatment, and prevention of vitamin D deficiency: an endocrine society clinical practice guideline. *J Clin Endocrinol Metab*. 2011;96:1911–30.

Publisher's note Springer Nature remains neutral with regard to jurisdictional claims in published maps and institutional affiliations.

Springer Nature or its licensor (e.g. a society or other partner) holds exclusive rights to this article under a publishing agreement with the author(s) or other rightsholder(s); author self-archiving of the accepted manuscript version of this article is solely governed by the terms of such publishing agreement and applicable law.